Response of Female and Male PMHS to Blast-Induced Vertical Accelerative Loading

Danielle M. Cristino[1], Hollie A. Pietsch[2], John H. Bolte IV[3], Andrew R. Kemper[1], Kerry A. Danelson[4], Warren N. Hardy[1]
[1]Center for Injury Biomechanics, Virginia Polytechnic Institute and State University, Blacksburg, VA; [2]U.S. Army Tank Automotive Research, Development and Engineering Center; [3]Injury Biomechanics Research Center, The Ohio State University, Columbus, OH; [4]Department of Orthopaedic Surgery, Wake Forest School of Medicine

ABSTRACT

Improvised explosive devices (IEDs) deliver a high energy blast to the underbody of military vehicles, consequently exposing modern Warfighters to considerable risk during ground transport. Biomechanical data are required to determine if a separate, operationally relevant anthropomorphic test device (ATD) suited for the assessment of risk associated with the female Warfighter should be developed, or if injury prediction outputs from the male ATD can be mapped to females. The objective of this study is to determine the differences between female and male impact and damage response in the under-body blast (UBB) environment. This study was conducted using the Accelerative Loading Fixture (ALF), which generates floor and seat loading conditions representative of UBB. Sixteen post-mortem human surrogates (PMHS) were tested, using two floor conditions. The PMHS tested include 50th percentile males, and 5th and 75th percentile females. The data obtained include the generalized kinematics of the distal tibia and femur, sagittal perspective planar segment motion, and PMHS lower extremity damage. The female and male tibia vertical acceleration and speed responses are similar in shape. All females attain greater speed earlier in the event. The 5th percentile female femurs attain greater acceleration earlier in the event during the lower-energy floor condition, while the 75th percentile female femurs attain greater acceleration during the higher-energy floor condition. The femur acceleration response of the female is notably shorter in duration, but similar in shape to the male response. The female lower extremities initially rotate in the sagittal plane at a higher rate than those of the males. Damage to the lower extremities was sustained during the higher-energy floor condition. Differences in damage response between sexes and percentiles are likely due to a combination of sex-related tolerance, anatomy, and mass phenomena. The results suggest that both the kinematics and damage response of female PMHS are markedly different than those of male PMHS.

INTRODUCTION

Improvised explosive devices deliver a high energy blast to the underbody of military vehicles, consequently exposing modern Warfighters to considerable risk during ground transport.

The UBB threat is characterized by high-rate accelerative loading in the vertical direction. This environment is fundamentally different than that seen in the civilian automotive domain and, as such, requires the development of specific tools to assess the environment, equipment, and injury outcome. The development and implementation of validated ATDs will lead to better prediction of risks associated with UBB and will aid in the design of improved vehicle systems and personal protection equipment. Previous work by Danelson et al. compared the impact and damage response of male PMHS to the Hybrid III ATD on the ALF. The results revealed that the ATD exhibits a stiffer overall response than PMHS, and that it is not well-suited for prediction of injury due to high-rate vertical loading (Danelson, 2015). The Warrior Injury Assessment Manikin (WIAMan), which is representative of a 50th percentile male, is the only ATD designed to evaluate injury patterns in UBB conditions (Pietsch, 2016). Injury assessment tools for the female Warfighter are not currently available. Therefore, injury countermeasures cannot be optimized with consideration for the female Soldier population. Collection of female PMHS UBB data is crucial for a better understanding of the distinct threat to the female Warfighter. The results of this ongoing study will ultimately lead to the development of either a female ATD for UBB, or appropriate, validated mapping schemes to apply to the existing WIAMan ATD. This study was designed to help determine the most effective course of future action. The focus of this research is the response of the lower extremity.

BACKGROUND

In an UBB event, the most significant injuries are those to the skeletal system. In a study of the Joint Theater Trauma Registry (JTTR), it was found that 1,566 Soldiers sustained 6,609 wounds as a result of enemy action during Operation Iraqi Freedom (OIF) and Operation Enduring Freedom (OEF) between October 2001 and January 2005 (Owens, 2008). A total of 3,575 (54.1%) of these wounds were to the extremities, with 915 (26%) of those being fractures (Owens, 2007).

Although lower extremity injuries from UBB are not always directly life-threatening, from a survivability standpoint, these results are of particular interest because they relate to the ability of the Warfighter to self-extricate and move to safety. In addition, injuries to the lower extremity can be debilitating, which can significantly decrease the quality of life and combat effectiveness of the Soldier. In the Owens study, 454 (50%) of the reported fractures were to the lower extremities, with the majority (48%) being to the tibia and fibula (Owens, 2007). Between October 2001 and June 2008, there were over 1,100 major limb amputations of U.S. Soldiers (Tintle 2010). In a more recent study, it was found that skeletal injuries to the leg and ankle make up 21% of the wounds reported in the Joint Trauma Analysis and Prevention of Injury in Combat (JTAPIC) database (Loftis, 2014). This reality has provided the impetus for researchers to study lower extremity response in an UBB environment, such as a recent study that examined the response of the foot and ankle complex to non-damaging vertical loading (Pintar, 2016).

Differences between female and male response to UBB is of increased importance as women in the armed services are integrated into additional military occupational specialties. As of August 2014, women comprised 16% of the total DoD force, however they accounted for 2.4% (113) of those killed in Iraq and Afghanistan since the beginning of OIF and OEF. During this

period, 32,799 U.S. service members were wounded in combat, with 606 of those being women (Powers, 2016). An important study examined the robustness and mechanical strength of the tibiae of a military population consisting of 442 women and 254 men. It was found that the tibiae of males are 40.9% stiffer than those of females, females have about 10% less cortical area relative to body size, and the tibiae of males are more robust, regardless of body size (Jepsen, 2011). To ensure protection of both female and male Soldiers, the female should be represented uniquely in test devices like ATDs or injury assessment criteria.

It is hypothesized that female PMHS will demonstrate notably different kinematics and damage mechanisms than male PMHS, and that damage to the female PMHS will occur at notably different injury tolerances than male PMHS. The purpose of this ongoing study is to determine what information and/or materiel are required to develop a valid injury assessment capability for female Soldiers in the UBB environment to better protect the full range of service members.

METHODS

Test Conditions and Surrogates

A total of 16 PMHS were tested in pairs. The input conditions to the seat and floor are defined by the target peak speed and the time taken to reach the specified peak speed (Table 1). Each test event is referred to as a "Shot." Test occupants are designated Crew 1 or Crew 2. The PMHS tested include 50th percentile males, and 5th and 75th percentile females (Table 2). In Series A, the first two tests involved male PMHS only (Shots with "M" in the designation), and the next four tests involved female PMHS or a 5th percentile ATD only (Shots with "F" in the designation). Although two tests involved an ATD, the focus of this study is PMHS response. In Series B, both females and males were tested in pairs. The 75th percentile females were comparable in stature and mass to the 50th percentile males. Test Series A implemented a lower-energy floor condition to collect kinematics data in the absence of substantive damage. Test Series B introduced a higher-energy floor condition to produce damaging test conditions. The lower extremity mass was measured for the PMHS in Series B (Table 3). The lower extremities were removed at the hip joint with the soft tissue being cut along the groin and gluteal furrow.

Table 1: Test matrix

Test Series	Shot	Peak Floor Speed	Floor Time-to Peak	Peak Seat Speed	Seat Time-to-Peak
A	M1, M2, F1, F2, F3, F4	8 m/s	2 ms	5 m/s	4 ms
B	F5, F6, F7	20 m/s	2 ms	4 m/s	7 ms

Table 2: Post-mortem human surrogate information

Shot	Crew	PMHS	Size	Sex	Age	Stature (cm)	Mass (kg)
M1	1	SM117	50th	Male	58	182.9	95.1
	2	SM118	50th	Male	54	174.5	82.5

M2	1	SM120	50th	Male	69	188.0	81.8
	2	SM119	50th	Male	73	181.8	65.0
F1	1	SF127	75th	Female	57	170.9	69.4
	2	SF126	5th	Female	54	159.2	47.2
F2	1	SF128	75th	Female	45	161.5	66.2
	2	ATD	5th	-	-	150.1	49.0
F3	1	SF131	75th	Female	55	165.1	68.5
	2	SF132	5th	Female	66	165.1	60.8
F4	1	SF133	5th	Female	57	162.6	57.4
	2	ATD	5th	-	-	150.1	49.0
F5	1	SF138	75th	Female	50	166.6	74.9
	2	SF134	5th	Female	53	171.6	60.7
F6	1	SM140	50th	Male	50	186.9	68.7
	2	SF135	5th	Female	36	160.3	56.9
F7	1	SM141	50th	Male	55	168.5	92.4
	2	SF142	75th	Female	75	164.3	80.8

Table 3: Lower extremity mass of PMHS in Series B

Shot	Crew	Size	Average Lower Extremity Mass (kg)
F5	1	F75th	9.15
	2	F5th	8.55
F6	1	M50th	8.55
	2	F5th	9.50
F7	1	M50th	6.60
	2	F75th	9.65

Test Apparatus

The Accelerative Loading Fixture (ALF) is a simplified representation of a military vehicle (Figure 1). It is designed to generate floor and seat loading conditions representative of the loading level, rate, location, direction, and extent seen in UBB. The ALF consists of two rigid seats mounted to a reinforced platform. The platform is explosively driven and travels upward within a superstructure frame. A brake system arrests its motion after it passes through the apex of its travel. The floor and seat performance can be modulated independently and are symmetric, predictable, and repeatable. The ALF was previously employed by Danelson, 2015, however modifications were made to stiffen the fixture and reinforce the seats for the desired loading in the current study.

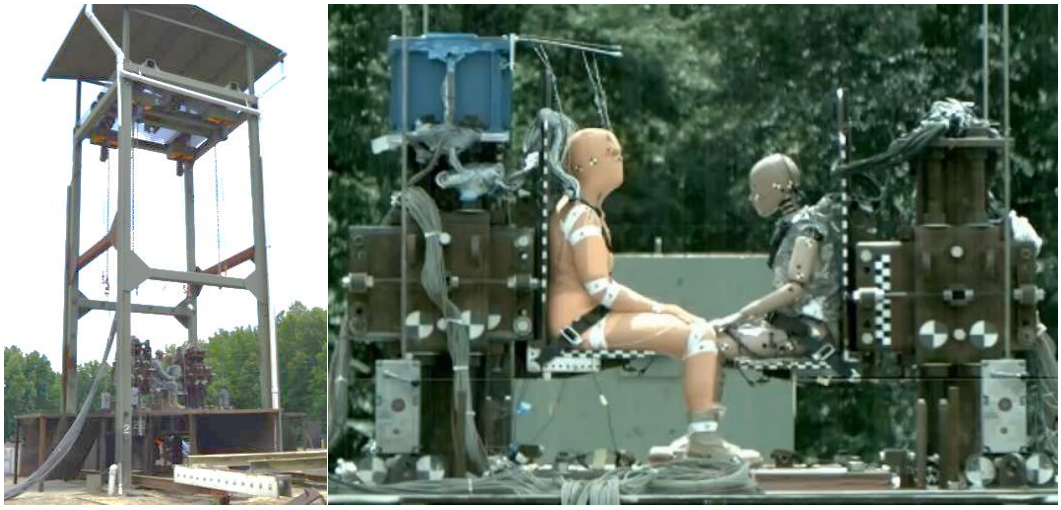

Figure 1: Accelerative Loading Fixture superstructure (left) and occupant platform (right).

Specimen Selection and Preparation

All PMHS underwent serologic screening and were examined for radiologic anomalies. PMHS were selected based upon sex, bone condition, mass, stature, and age (Table 4). Comprehensive x-rays and anthropometry were collected. Strain gages were adhered to the anterior aspect of the distal and proximal tibiae and femurs (Micro-Measurements cea-06-250uw-350), as well as the calcanei (Micro-Measurements cea-13-062uw-350). Accelerometers (Endevco 7264, 7264B, or 7264C) and angular rate sensors (DTS ARS Pro or HG) were arranged into six-degree-of-freedom motion blocks consisting of three orthogonal linear accelerometers and three angular rate sensors. The motion blocks were rigidly mounted to the distal tibiae and femurs, bilaterally. Pre-test computed tomography (CT) scans documented the position and orientation of the instrumentation.

Table 4: Specimen anthropometric inclusion criteria

PMHS	Anthropometry	Minimum	Maximum
50th Male	Stature (cm)	165	186
	Mass (kg)	64	106
75th Female	Stature (cm)	160.9	173.7
	Mass (kg)	64	89
5th Female	Stature (cm)	145.6	158.4
	Mass (kg)	39	63
All	BMI	18	35
	BMD (T-Score)	-1.0	+2.5
	Age	18	80

Test Procedure

PMHS were fitted with boots, seated on the ALF, and secured using five-point restraints. Video tracking targets were placed on the PMHS to define body segments and important

anatomical landmarks. The PMHS were positioned according to the WIAMan Bio PT PMHS Positioning Procedure guidelines (Rupp, 2015). A portable coordinate measurement machine (FARO) was used to characterize and set the three-dimensional location of relevant anatomical landmarks. Instrumentation and video cameras were verified and trigger checks were completed before the charge was placed and the shot was conducted. After the test, CT scans were obtained and comprehensive autopsies were performed.

Data Collection and Analysis

The data obtained include generalized kinematics of the distal tibia and femur, sagittal perspective planar segment motion, and lower extremity damage results. There were two data acquisition systems for each PMHS. The first was a 32 channel DTS G5 sampled at 100 kHz, with a 30 kHz cutoff, 8^{th} order Butterworth profile, low-pass filter. The second was a 64 channel DTS TDAS Pro sampled at 20 kHz with a 4,300 Hz cutoff, 8^{th} order Butterworth profile, anti-aliasing filter. Coordinate system transformations of the transducer data were performed to align the signals with the anatomical axes and to coincide with defined anatomical origins (Miller, 2015). The data were corrected for polarity then zeroed, truncated, and filtered. Linear acceleration was filtered using a cutoff frequency of 3 kHz and angular rate was filtered using a cutoff frequency of 1.65 kHz. Angular acceleration was calculated by differentiating angular speed and filtered using 0.5 kHz cutoff. All filters were 4^{th}-order Butterworth profiles (Miller, 2015). Video was recorded using Photron FASTCAM SA1.1 cameras operating at 10 kfps.

RESULTS

Impact Response

Tibia. In Series A and B, the female tibia vertical speed responses are similar in shape and duration to those of the males (Figures 2 and 3). In Series A, the females attained greater speed earlier in the event (Figure 2). The female tibiae have greater initial vertical acceleration in Series A (Figure 4). These trends were not observed in Series B (Figures 3 and 5). The tibia speeds in Series B were twice those of Series A.

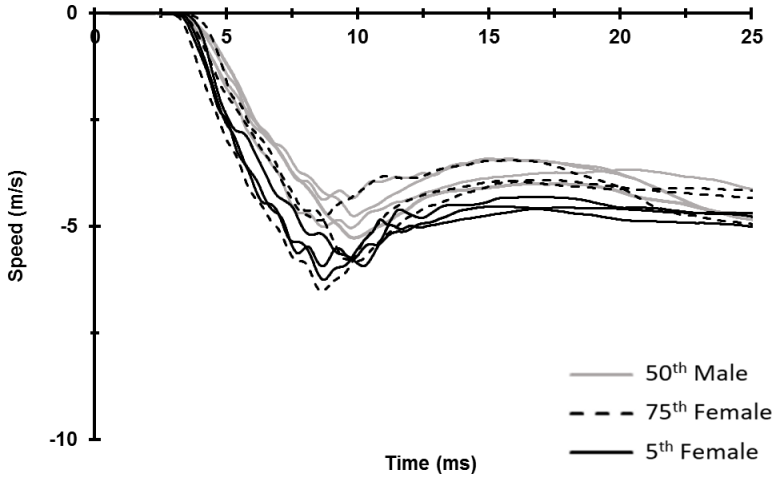

Figure 2: Series A - left distal tibia vertical speed.

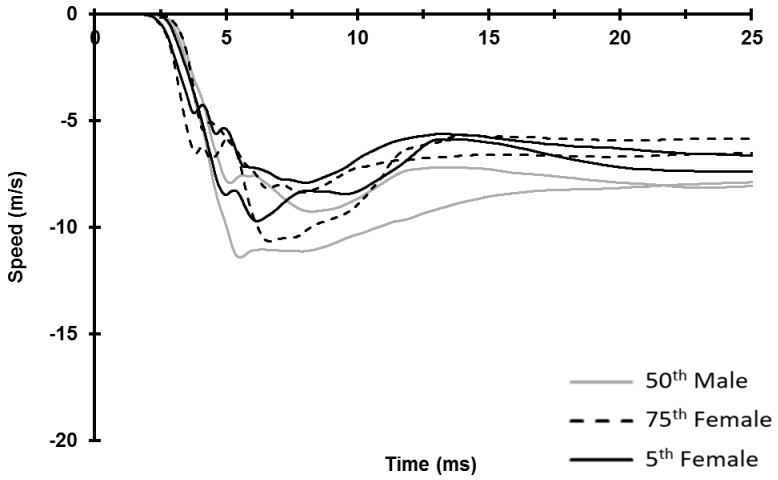

Figure 3: Series B - right distal tibia vertical speed.

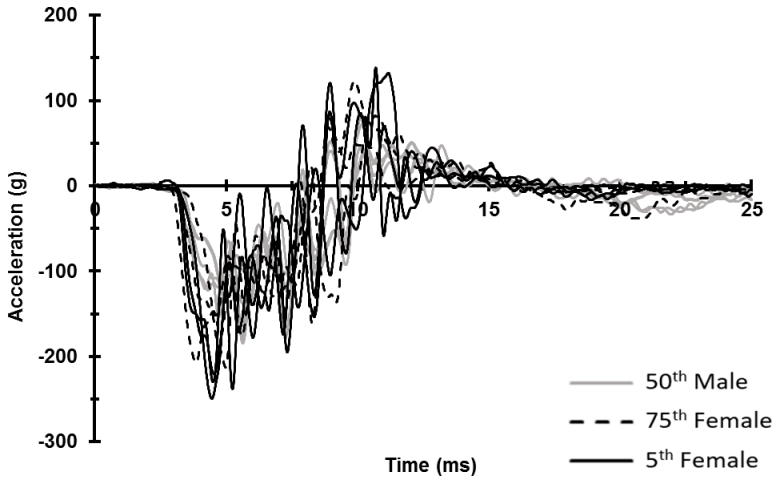

Figure 4: Series A - left distal tibia vertical acceleration.

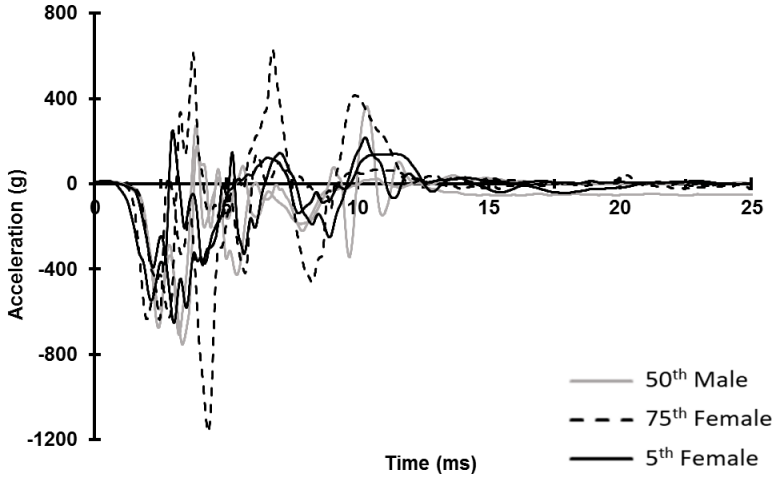

Figure 5: Series B - left distal tibia vertical acceleration.

Femur. In Series A, the female and male femur vertical speed responses were similar in shape, with the females attaining a greater peak speed earlier in the event (Figure 6). This trend was not observed in Series B (Figure 7). In Series A, the 5th percentile females had shorter acceleration duration and larger vertical accelerations earlier in the event (Figure 8). In Series B, the 75th percentile female initial acceleration magnitudes were higher (Figure 9).

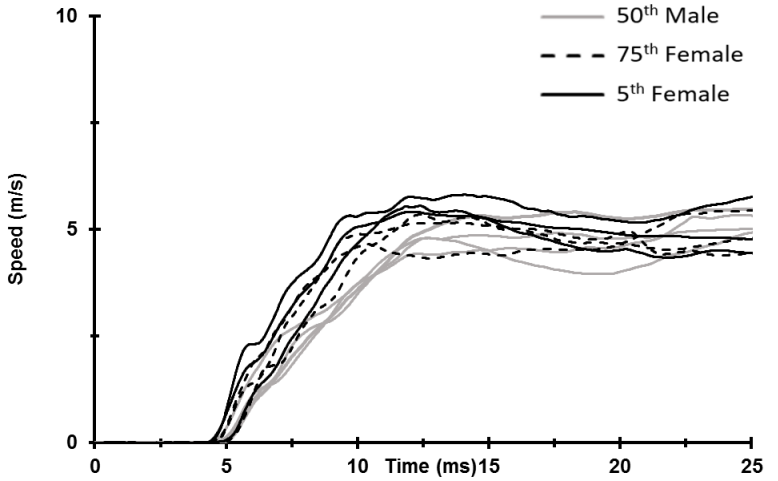

Figure 6: Series A - right distal femur vertical speed.

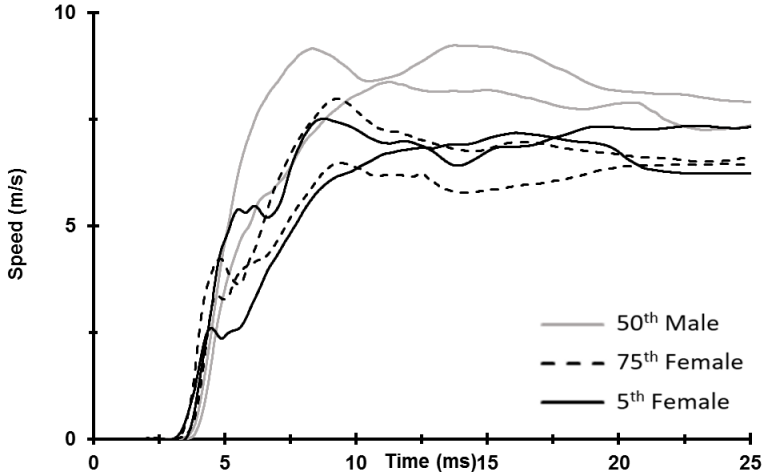

Figure 7: Series B - right distal femur vertical speed.

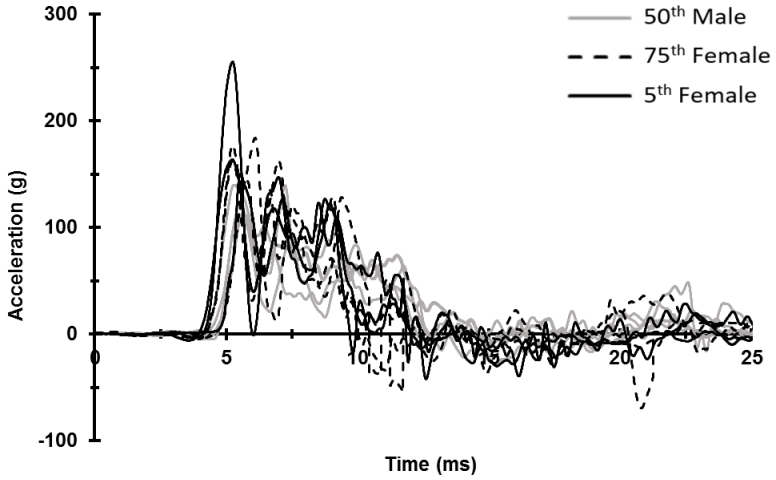

Figure 8: Series A - right distal femur vertical acceleration.

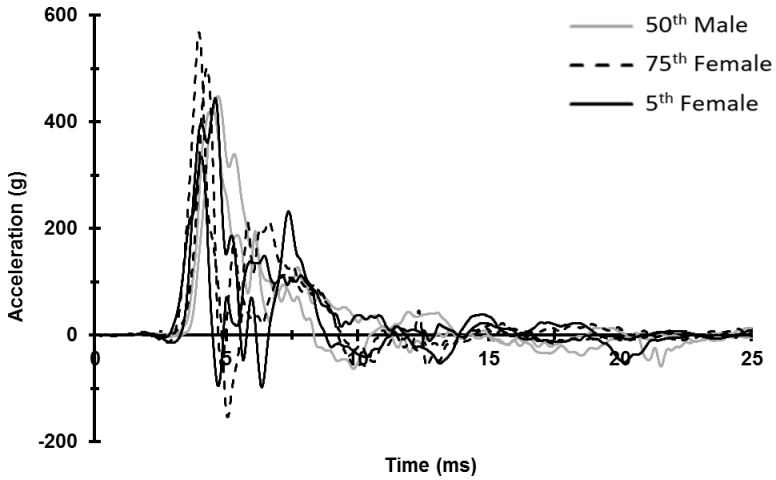

Figure 9: Series B - right distal femur vertical acceleration.

Femur Rotation. In Series A, the rotation of the femurs in the sagittal plane is similar in shape for the females and males, but the female specimens initially rotate faster (and more) than the 50th percentile males (Figure 10). In Series B, the femurs of the 75th percentile females and 50th percentile males maintain higher angular speed for a longer period (Figure 11).

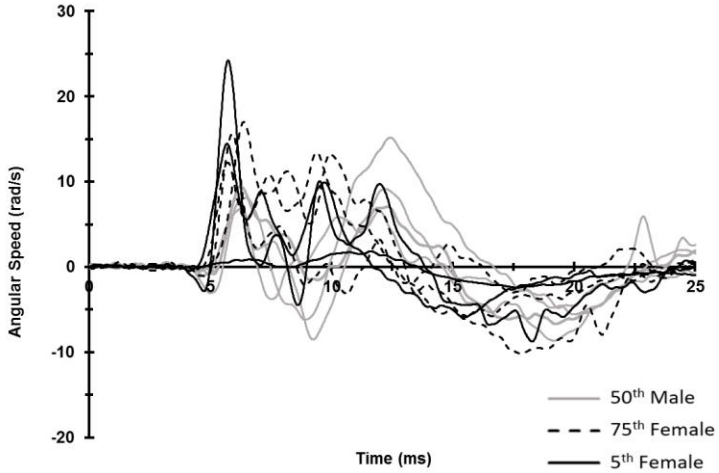

Figure 10: Series A - right distal femur angular speed about the y-axis.

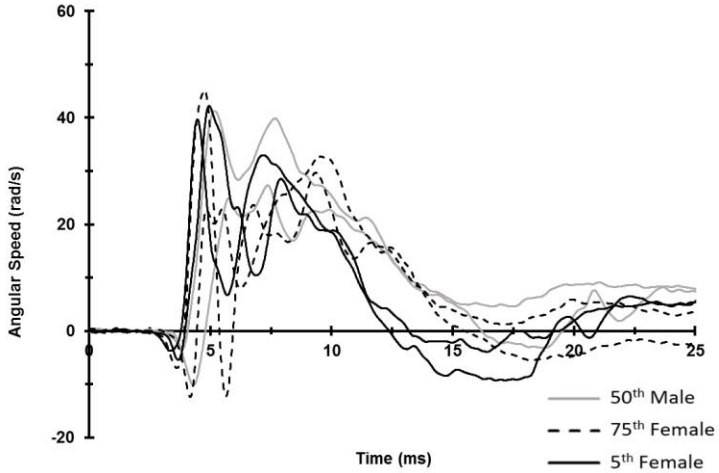

Figure 11: Series B - right distal femur angular speed about y-axis.

Fracture Timing. Strain gage data provide insight into fracture timing. The time at which there is an initial sharp transition in strain is assumed to indicate the onset of damage (Danelson, 2015). Estimated times of fracture initiation with respect to the onset of lower extremity motion are summarized for the calcaneus, distal tibia, and proximal femur in Table 5 for Series B. A sample plot of both femur fractures, which occur near ten milliseconds, is provided in Figure 12.

Table 5: Series B fracture initiation time (ms) with respect to the onset of lower extremity motion

		Calcaneus		**Distal Tibia**		**Proximal Femur**	
Shot	Crew	Right	Left	Right	Left	Right	Left
F5	1	1.8	-	3.5	2.0	-	-
	2	No Signal	1.6	-	1.5	-	8.7

F6	1	2.6	2.7	-	-	-	7.3
	2	2.4	1.4	-	-	-	-
F7	1	-	2.1	-	-	-	-
	2	2.4	1.3	-	1.0	-	-

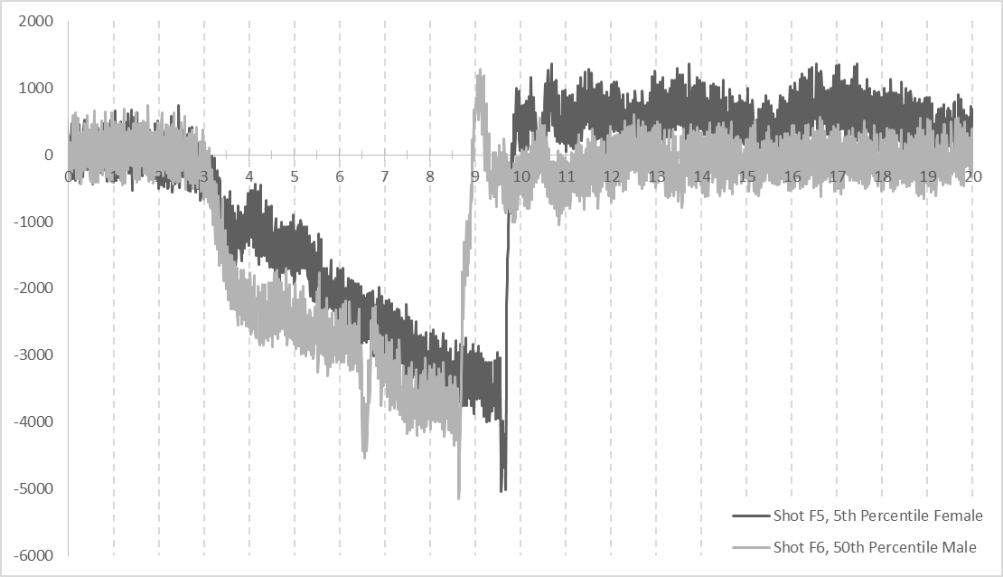

Figure 12: Strain output vs. time (ms) for femurs that sustained fractures.

Damage Response

A detailed damage summary is included in Appendix A. The only instance of lower extremity damage in Series A was a partial neck fracture of the left talus of a 5th percentile female. The increased floor energy in Series B resulted in damage throughout the lower extremities, which is summarized in Table 6. Minor damage to the right or left side is indicated by "rt." or "lt.", respectively. Major damage is indicated by "**Rt**." or "**Lt**." Damage was considered major when the structural integrity of the bone was compromised.

Table 5: Lower extremity damage response in Series B

Shot	Crew	Femur	Tibia	Fibula	Talus	Calcaneus	Navicular	Cuboid	Forefoot
5	1 (75th Female)		rt./**Lt**.	**Lt**.	rt.	**Rt**.	rt./lt.	rt./ lt.	lt.
	2 (5th Female)	**Lt**.	lt.		**Rt**.	**Rt**./ **Lt**.	lt.		lt.
6	1 (50th Male)	**Lt**.				**Rt**./**Lt**.			lt.
	2 (5th Female)				lt.	**Rt**./**Lt**.	rt.		
7	1 (50th Male)					**Lt**.			
	2 (75th Female)		**Lt**.	**Lt**.	rt./lt.	**Rt**./**Lt**.	rt.		

Midfoot and Forefoot. Series B induced damage in the midfoot and forefoot. All of the female and none of the male PMHS sustained some form of midfoot damage. There were five cases of damage to the navicular, with four being fractures similar to the one shown in Figure 13. All navicular damage was to the lateral and inferior aspect of the bone. The two observed cuboid fractures were associated with navicular fractures (Figure 13). There were three metatarsal fractures, one each on a 5th and 75th percentile female, and a 50th percentile male (Figure 14). There was one phalange fracture on a 75th percentile female. All damage to bones of the forefoot occurred at the proximal end.

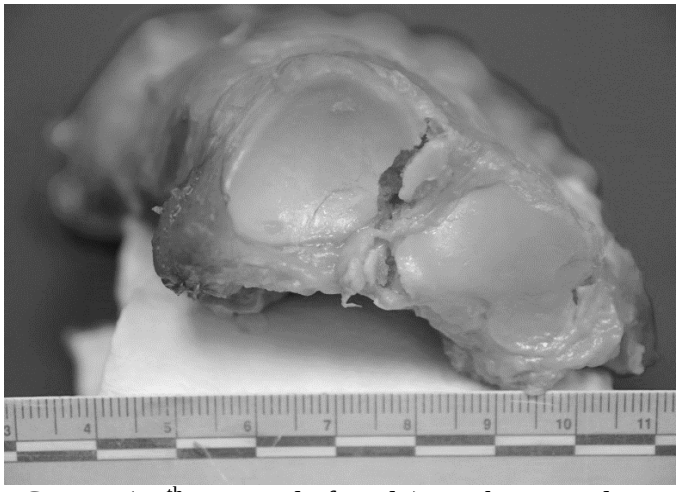

Figure 13: Shot F5, Crew 1 (75th percentile female) - right navicular and cuboid fractures.

Figure 14: Shot F6, Crew 1 (50th percentile male) - left proximal 4th metatarsal fracture.

Calcaneus. In Series B, all PMHS sustained damage to either one or both calcanei. Four cases were bilateral. Unilateral damage was observed in one 75th percentile female on the right side and one 50th percentile male on the left side. There were two observed fracture modes for the calcaneus: crushed and sectioned (Figure 15). The two calcanei that were sectioned belonged to specimen that were heavier than almost all other specimen.

Figure 15: Shot F5, Crew 2 (5th percentile female) - crushed left calcaneus (left photo); Shot F7, Crew 1 (50th percentile male) - sectioned left calcaneus (right photo).

Talus. In Series A, minor talus damage was sustained by one 5th percentile female. In Series B, all females sustained talus damage and no males sustained talus damage. Minor damage was sustained by one 5th percentile female (Figure 16) and one 75th percentile female. Major damage was sustained by a different 5th percentile female (Figure 17). Both minor and major damage was sustained by another 75th percentile female.

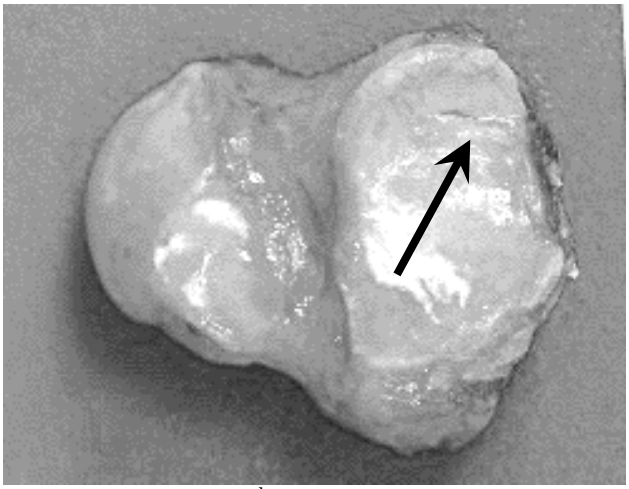

Figure 16: Shot F6, Crew 2 (5th percentile female) - left talus fracture.

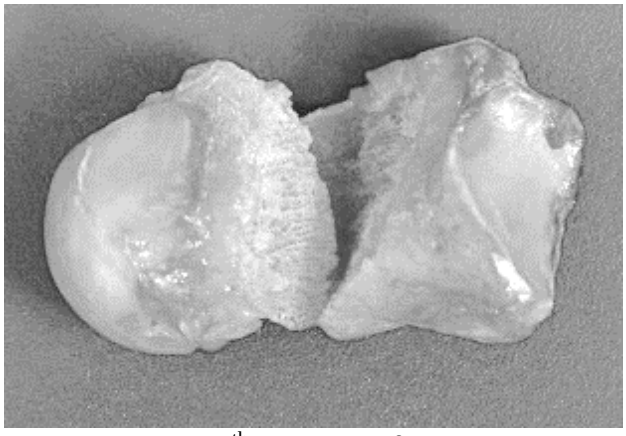

Figure 17: Shot F5, Crew 2 (5th percentile female) - sectioned right talus.

Tibia and Fibula. In Series B, three female PMHS sustained damage to the distal tibia. One 5th percentile female sustained a pilon fracture of the left distal tibia. One 75th percentile female sustained a shattered left distal tibia (Figure 18). A second 75th percentile female sustained a pilon fracture to the right distal tibia (Figure 19) and a compression fracture of the left distal tibia. Both cases of severe damage to the distal tibia occurred on the left side of 75th percentile females and had concomitant fibula fractures (Figure 20). No male sustained tibia or fibula damage.

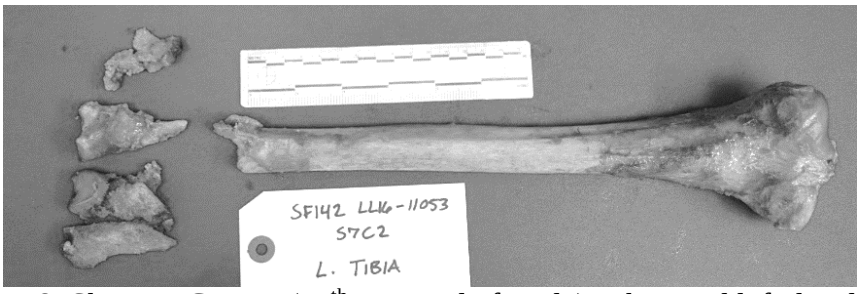

Figure 18: Shot F7, Crew 2 (75th percentile female) - shattered left distal tibia.

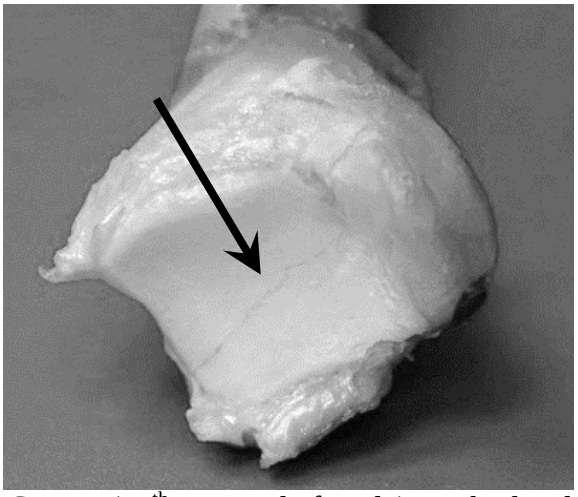

Figure 19: Shot F5, Crew 1 (75th percentile female) - right distal tibia pilon fracture.

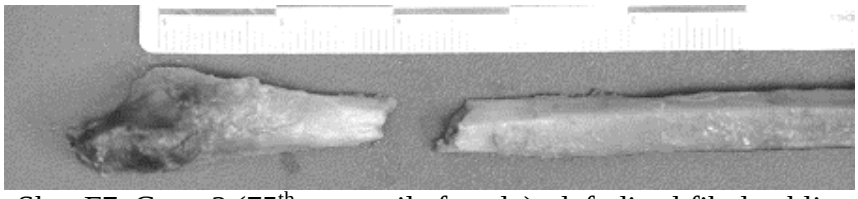

Figure 20: Shot F7, Crew 2 (75th percentile female) - left distal fibula oblique fracture.

Femur. In Series B, one male and one 5th percentile female PMHS sustained a femur fracture. The male sustained a spiral wedge fracture of the left femur due to a combination of bending and torsion (Figure 21). The 5th percentile female sustained a segmented bending fracture of the left femur that resulted from bending, with torsion being a possible contributor (Figure 22).

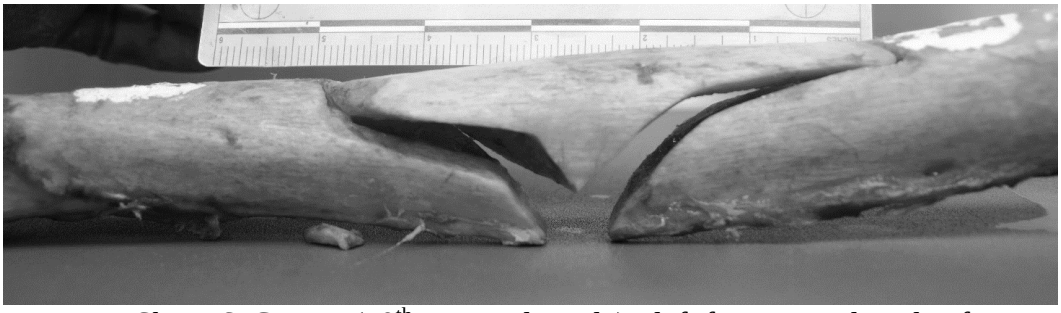

Figure 21: Shot F6, Crew 1 (50th percentile male) - left femur spiral wedge fracture.

Figure 22: Shot F5, Crew 2 (5th percentile female) - left femur segmented bending fracture.

DISCUSSION

Kinematics Response

The femur acceleration response of both the females and males in Series A exhibited an oscillatory square unimodal response. In Series B, the heavier lower extremities of the female PMHS exhibited a second-order effect in the vertical speed response of the femur. The associated female acceleration responses were triangular and bimodal in nature, in contrast to those observed during Series A.

Initial interpretation of the results from Series A and B suggests that the kinematics response of the female PMHS is different from the male PMHS. The primary measured difference is that the female PMHS attain a higher velocity at an earlier time for the lower extremities. This finding is considered to be due to differences in size or mass, not anatomy nor shape. Furthermore, heavier lower extremities require increased energy input to overcome inertial resistance to movement. This results in increased contact time between the boot and the floor, which leads to greater energy transfer to the load bearing structures of the lower extremity. As a result, the extent of damage to the lower extremities might be influenced by mass.

Due to the nature of the floor deformation, the duration of contact between the floor and the left foot was shorter than the right foot, which suggests greater energy transfer sooner in the event. Severe damage to the lower extremity tended to occur more proximally on the left side than on the right side, which suggests that there is a relationship between contact duration and damage response.

Damage Response

The most frequent type of severe damage was a crushed calcaneus; however, in two cases, the most severe damage was to the distal leg. This damage was associated with a sectioned calcaneus in one case and no damage to the calcaneus in the other case. Thus, in the absence of severe damage to the calcaneus, the distal bones of the leg were catastrophically damaged. Accordingly, when the calcaneus was crushed, the damage proximal to the calcaneus was less severe. In these cases, damage to the talus was severe when the distal leg was undamaged, while minor damage to the distal leg was associated with an intact or minimally damaged talus. Damage to the talus did not occur in the absence of damage to the calcaneus, and was never more severe than that of the calcaneus. Further, talus fractures occurred in the absence of damage to the distal tibia (three cases), suggesting that it is possible to have sustained loading of the talus without the distal tibia failing first. Within these tests, damage to the distal tibia occurred when there was no damage to the talus bone (three cases). These differences might be due to tolerance or bone size.

Fracture of the left femur occurred in both a male and a female PMHS. Both occupants had comparatively lower mass lower extremities. The 50^{th} percentile male sustained a spiral wedge fracture, which resulted from a combination of bending and torsion. The torsional component potentiated this damage, which resulted from inertia of the thigh. The 5^{th} percentile female sustained a segmented bending fracture. It is possible that combined higher acceleration and lower bone strength could have made an inertial fracture more likely for the female, even in the absence of appreciable torsion. The female had relatively lower mass lower extremities and relatively higher peak vertical femur acceleration. This suggests that reduced tolerance could be a factor in this unlikely fracture.

There were several notable differences in damage response between the female and male PMHS. Three female PMHS incurred tibia damage and both 75^{th} percentile females sustained concomitant fibula fractures. No males sustained tibia or fibula damage. During Series B, all females sustained some form of talus damage, while no talus damage was found in any males. All of the female and none of the male PMHS in Series B sustained some form of midfoot damage. These differences may be due to lower female tolerance levels or higher lower extremity mass. In

the case of the latter, differences in weight distribution between females and males may be an important consideration.

CONCLUSIONS

The results presented herein suggest that both the kinematics and damage response of female PMHS are different from male PMHS. The primary measured difference is that the female PMHS attain a higher velocity at an earlier time for the lower extremities. Damage differences are due to a combination of sex-related tolerance, anatomy, and mass phenomena. These differences need to be investigated further using additional tests on the ALF, as well as component testing to determine if there are differences in fracture morphology or tolerance between females and males. At this time, the development of a female ATD may be needed for UBB if occupant kinematics are required to develop injury countermeasures. However, additional testing would be required to confirm this conclusion. If kinematics are not considered critical, an extensive investigation into female response for a range of percentiles could be conducted to develop validated mapping schemes between the existing WIAMan ATD and the female Warfighter.

ACKNOWLEDGMENTS

This work was funded through the WIAMan Engineering Office of the Army Research Laboratory under Award Number W911NF-14-2-0023.

REFERENCES

DANELSON, K.A., KEMPER, A.R., MASON, M.J., TEGTMEYER, M., SWIATKOWSKI, S.A., BOLTE, J.H., HARDY, W.N. (2015). Comparison of ATD to PMHS Response in the Under-Body Blast Environment. 59th Stapp Car Crash Conference, pp. 445-520.

JEPSEN, K.J., CENTI, A., DUARTE, G.F., GALLOWAY, K., GOLDMAN, H., HAMPSON, N., LAPPE, J.M., CULLEN, D.M., GREEVES, J., IZARD, R., NINDL, B.C., KRAEMER, W.J., NEGUS, C.H., EVANS, R.K. (2011). Biological Constraints That Limit Compensation of a Common Skeletal Trait Variant Lead to Inequivalence of Tibial Function Among Healthy Young Adults. Journal of Bone and Mineral Research 26(12): 2872-2885.

LOFTIS, K.L., GILLICH, P.J. (2014). Trauma Comparison of Civilian Automotive with Military Combat Injuries. Short Communications from AAAM's 58th Annual Scientific Conference. Traffic Injury Prevention 15(sup1): S238-S269.

MILLER, C., RUPP, J., HUMM, J., ALAI, A., KANG, Y.S., DOOLEY, C., SHERMAN, D., MARCUS, I., BIGLER, B. Signal Conversion Tiger Team [ScoTT] Recommendations for Anatomical Reference Rev. 0.6 May 21, 2015 (under review).

OWENS, B.D., KRAGH, J.F., MACAITIS, J., SVOBODA, S.J., WENKLE, J.C. (2007). Characterization of Extremity Wounds in Operation Iraqi Freedom and Operation Enduring Freedom. J Orthop Trauma 21(4): pp. 254-257.

OWENS, B.D., KRAGH, J.F., WENKLE, J.C., MACAITIS, J., WADE, C.E., HOLCOMB, J.B. (2008). Combat Wounds in Operation Iraqi Freedom and Operation Enduring Freedom. J Trauma 64(2): 295-299.

PIETSCH, H.A., BOSCH, K.E., WEYLAND, D.R., SPRATLEY, E.M., HENDERSON, K.A., SALZAR, R.S., SMITH, T.A., SAGARA, B.M., DEMETROPOULOS, C.K., DOOLEY, C.J., MERKLE, A.C. (2016). Evaluation of WIAMan Technology Demonstrator Biofidelity Relative to Sub-Injurious PMHS Response in Simulated Under-body Blast Events. 60th Stapp Car Crash Conference, pp. 199-246.

PINTAR, F.A., SCHLICK, M.B., YOGANANDAN, N., VOO, L., MERKLE, A.C., KLEINBERGER, M. (2016). Biomechanical Response of Military Booted and Unbooted Foot-Ankle-Tibia from Vertical Loading. 60th Stapp Car Crash Conference, pp. 247-285.

POWERS, R. (2016). The Cost of War. Retrieved from: thebalance.com.

RUPP, J., REED, M. WIAMan Bio PT PMHS Positioning Procedure guidelines. Rev. 0.7 Dec 9, 2015 (under review).

TINTLE, S.M., FORSBERG, J.A., KEELING, J.J., SHAWEN, S.B., POTTER, B.K. (2010). Lower Extremity Combat-Related Amputations. Journal of Surgical Orthopaedic Advances 19(1): 35-43.

APPENDICES

Appendix A: Detailed lower extremity damage list

Shot F4, Crew 1

- Lt. talus partial neck fx

Shot F5, Crew 1

- Rt. distal tibia, pilon fx
- Rt. calcaneus, crushed
- Rt. talus, chip on posterior facet and head

- Rt. navicular, fx through lateral/inferior corner
- Rt. cuboid, fx of lateral edge of articular surface for calcaneus
- Lt. distal tibia, compression fx
- Lt. distal fibula, vertical fx of lateral malleolus
- Lt. navicular, fx through lateral/inferior corner
- Lt. cuboid, chip on lateral/distal corner
- Lt. 5th proximal metatarsal, crushed
- Lt. 4th proximal metatarsal, chip
- Lt. 5th proximal phalanx, fx

Shot F5, Crew 2

- Rt. calcaneus, crushed
- Rt. talus, separated body
- Lt. femur, segmented bending fx (spaghetti fx)
- Lt. tibia, pilon fx
- Lt. calcaneus, crushed
- Lt. navicular, fx through lateral/inferior corner
- Lt. proximal 5th metatarsal, fx

Shot F6, Crew 1

- Rt. calcaneus, crushed
- Lt. femur, spiral wedge fx (Müller AO 32-B1.2)
- Lt. calcaneus, crushed
- Lt. proximal 4th metatarsal, fx

Shot F6, Crew 2

- Rt. calcaneus, crushed
- Rt. navicular, damage to lateral aspect of articular surface for talus
- Lt. calcaneus, crushed
- Lt. talus, fx of posterior facet

Shot F7, Crew 1

- Lt. calcaneus, sectioned

Shot F7, Crew 2

- Rt. Calcaneus, crushed
- Rt. Talus, posterior facet fx and trochlea fx
- Rt. Navicular, fx through lateral/inferior corner
- Lt. calcaneus, sectioned
- Lt. talus, cartilage damage to head
- Lt. distal tibia, shattered
- Lt. fibula, oblique fx of diaphysis of distal end, separation of head

Appendix B: Peak accelerations and speeds for distal tibia and distal femur of all PMHS in Series A and B

Table B1: Peak accelerations and speeds

		Peak Vertical Acceleration (g)				Peak Vertical Velocity (m/s)			
Shot	PMHS	Rt. Fem.	Lt. Fem.	Rt. Tib.	Lt. Tib.	Rt. Fem.	Lt. Fem.	Rt. Tib.	Lt. Tib.
M1 Crew 1	50th male	122	140	-155	-125	5	5	5	5
M1 Crew 2	50th male	140	116	-189	-179	5	5	-5	-5
M2 Crew 1	50th male	139	112	-147	-185	5	5	-5	-5
M2 Crew 2	50th male	113	126	-137	-139	5	5	-6	-5
F1 Crew 1	75th female	163	174	-234	-208	5	6	-6	-7
F1 Crew 2	5th female	164	416	-219	-239	5	6	-5	-6
F2 Crew 1	75th female	177	150	-213	-152	5	5	-5	-5
F3 Crew 1	75th female	184	144	-274	-213	5	6	-5	-6
F3 Crew 2	5th female	150	245	-244	-250	6	7	-5	-6
F4, Crew 1	5th female	255	189	-320	-221	6	6	-6	-6
F5 Crew 1	75th female	567	528	-685	-635	8	7	-8	-8
F5 Crew 2	5th female	335	-1292	-434	-547	7	9	-8	-12
F6 Crew 1	50th male	421	2107	-565	-709	8	14	-9	-13
F6 Crew 2	5th female	444	494	-544	-651	8	10	-10	-12
F7 Crew 1	50th male	448	772	-684	-753	9	9	-11	-91
F7 Crew 2	75th female	501	477	-745	-1163	6	7	-11	-13

Appendix C: Frames from Shot F5 (Figure C1) and Shot F6 (Figure C2).

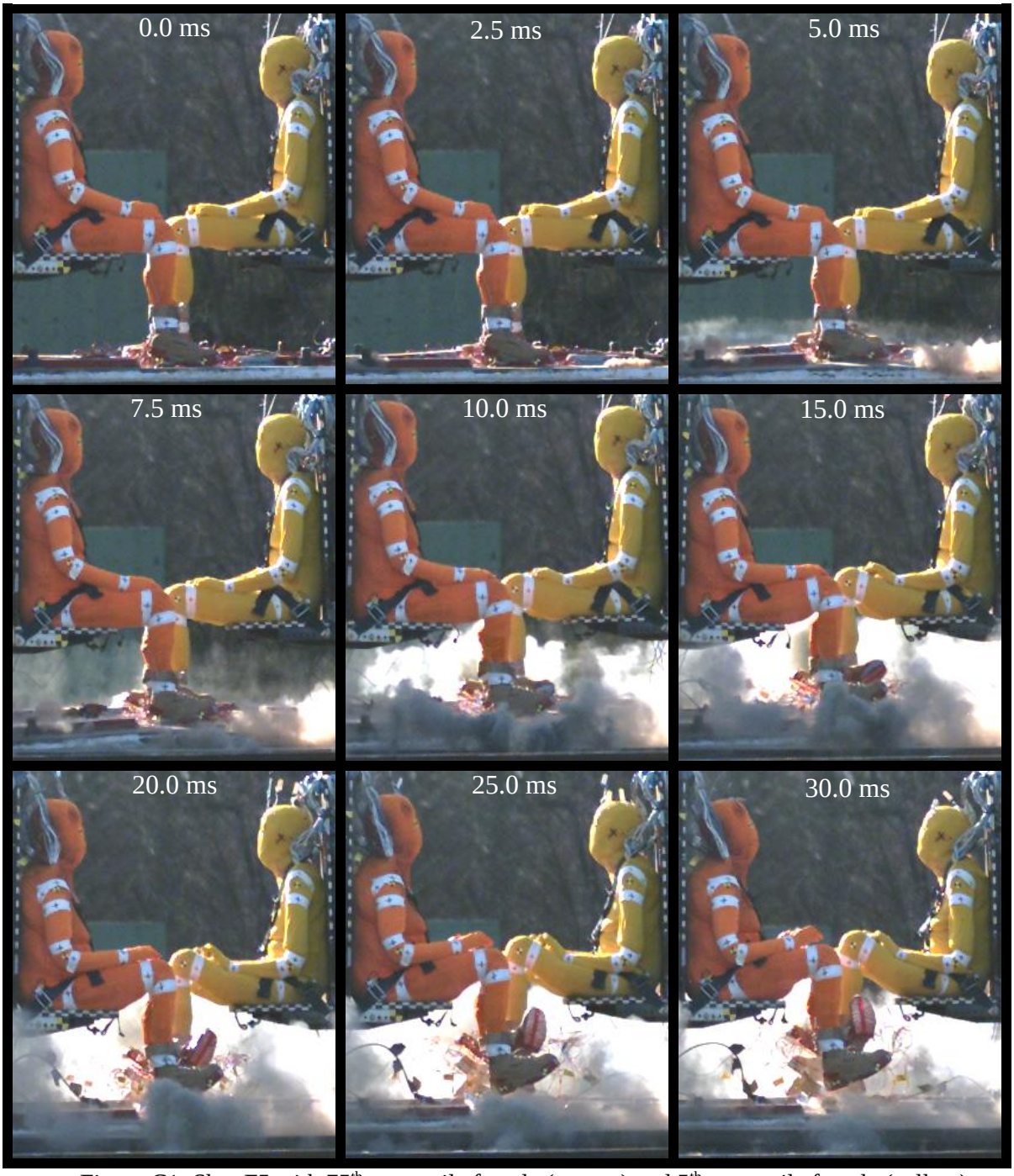

Figure C1: Shot F5 with 75th percentile female (orange) and 5th percentile female (yellow).

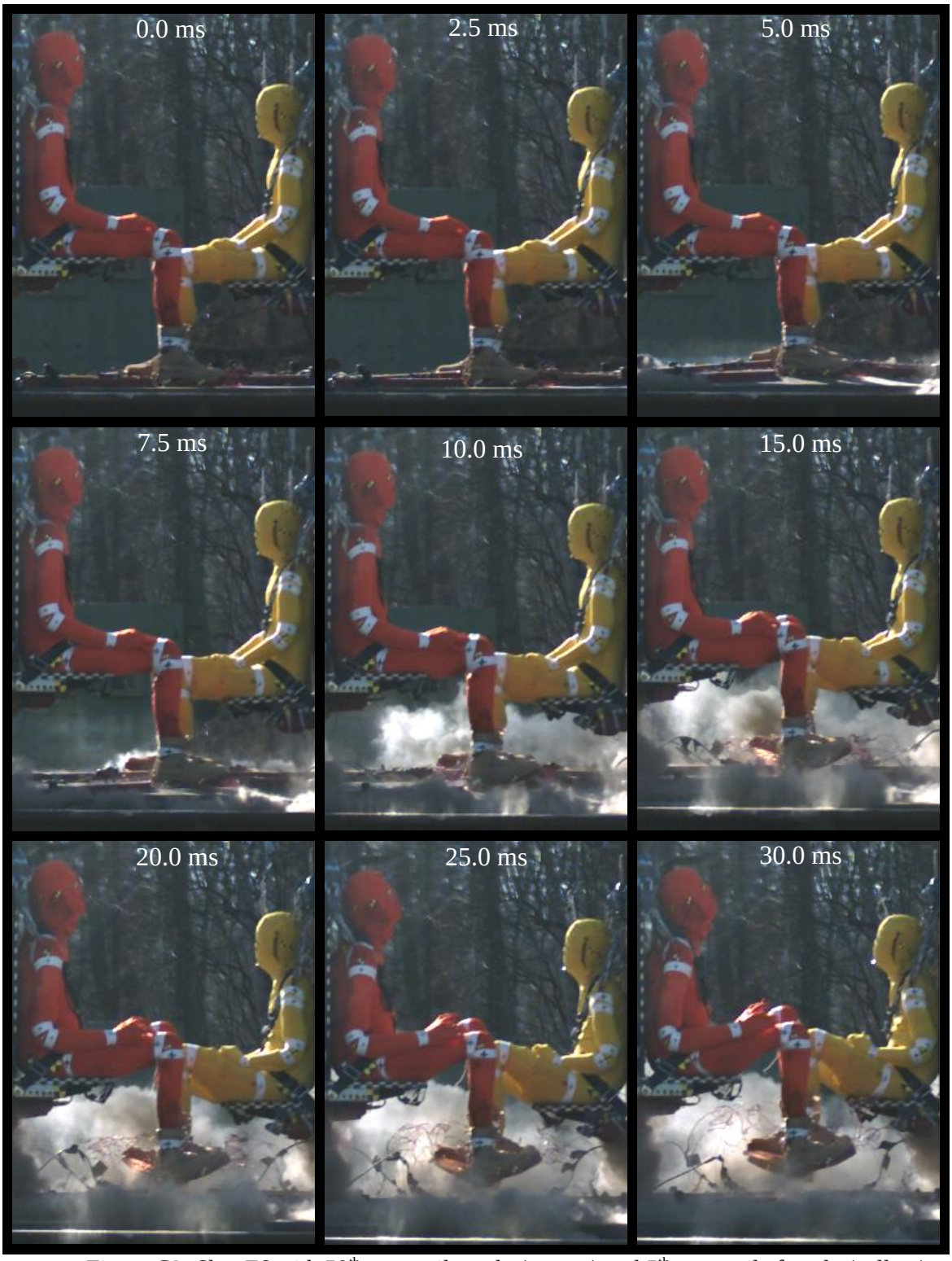

Figure C2: Shot F6 with 50th percentile male (orange) and 5th percentile female (yellow).